14th International Workshop on e+e− Collision from Phi to Psi 2026

Pisa, 8-11 June 2026

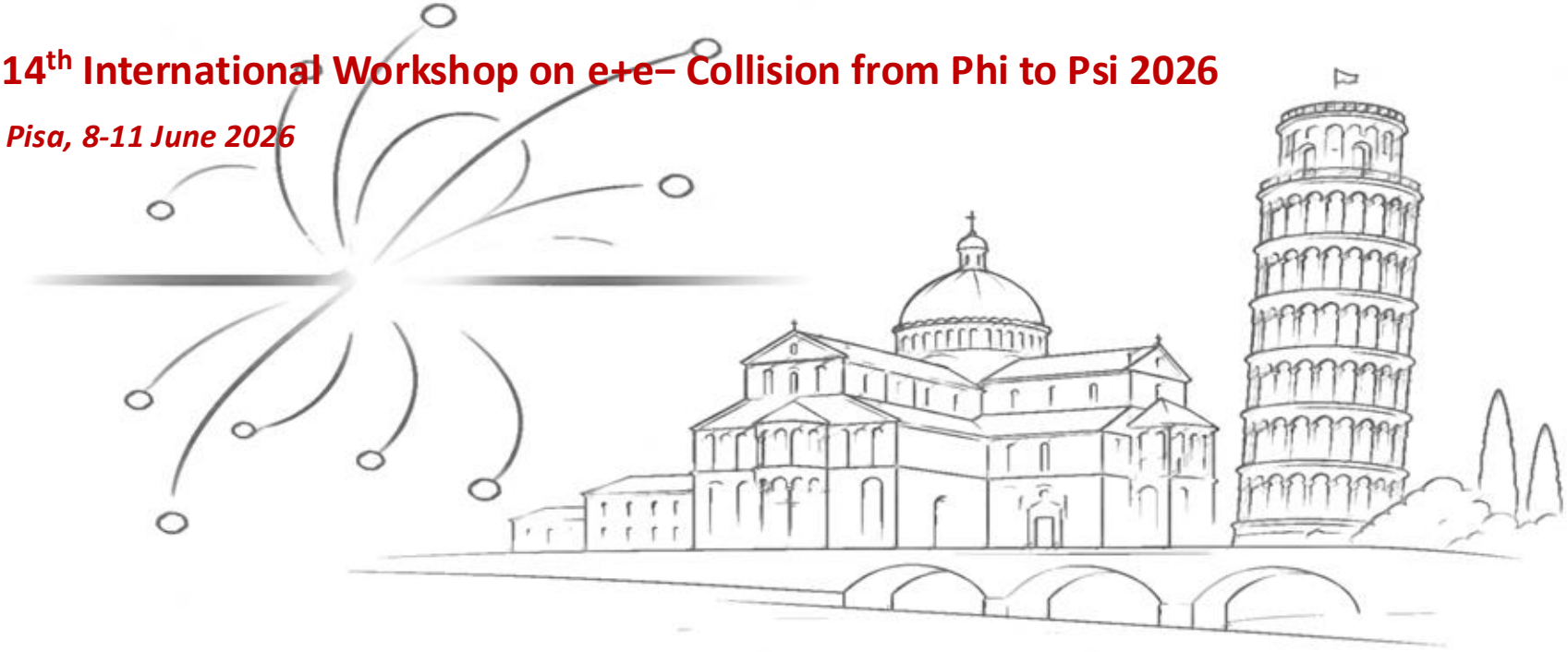

New Precise Measurement of the $e^+e^- \to \pi^+\pi^-$ Cross Section with BABAR for g-2 Calculation

I. Garzia
on behalf of BaBar Collaboration

garzia@fe.infn.it
isabella.garzia@unife.it

OUTLINE

- Introduction
- The BaBar experiment and data set
- 2009 vs 2025 new analysis procedure
- Overview of Analysis procedure
  1. Kinematic fits
  2. Angular fits
  3. μμγ spectrum comparison to QED prediction
  4. Determination of ISR luminosity
  5. $e^+e^- \to \pi^+\pi^-(\gamma)\gamma_{ISR}$ cross section
  6. Comparison with 2009 BaBar results and contributions to a_μ
- Summary and conclusions

Introduction: Anomalous Magnetic Moment and Hadron Vacuum Polarization

The anomalous magnetic moment of the muon (a_μ) is one of the most precisely predicted and measured observables in particle physics

$$a_\mu = \frac{(g-2)_\mu}{2}$$

Dirac predicted g = 2 for electrons in 1928
[Proc. Roy. Soc. Lond. A 118, 351]

In SM calculation:

$$a_\mu^{\mathrm{SM}} = a_\mu^{\mathrm{QED}} + a_\mu^{\mathrm{had}} + a_\mu^{\mathrm{EW}}$$

0,001 ppm ⊕ 0,37 ppm ⊕ 0,01 ppm

$$a_\mu^{\mathrm{HVP,\,LO}} = \left(\frac{\alpha m_\mu}{3\pi}\right)^2 \int_{s_{\mathrm{thr}}}^{\infty} ds \frac{\hat{K}(s)}{s^2} R_{\mathrm{had}}(s)$$

$$R_{\mathrm{had}}(s) = \frac{3s}{4\pi\alpha^2}\sigma[e^+e^- \to \mathrm{hadrons}(+\gamma)]$$

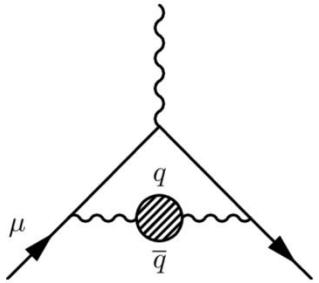

HVP
Hadronic Vacuum Polarisation

Hadronic vacuum polarization (HVP) contribution to $\mathbf{a}_\mu$ can be obtained by measuring cross sections of $e^+e^- \to$ hadrons

- largest input from $e^+e^- \to \pi^+\pi^-$ (73%)
- also calculated with Lattice QCD

$a_\mu^{\mathrm{HVP,LO}}$ data-driven prediction has the largest uncertainty ➔ The focus of the study

Introduction: Anomalous Magnetic Moment and Hadron Vacuum Polarization

Current **tensions** exist between:

- predictions from dispersion approach and direct measurement;
- predictions from dispersion approach and lattice QCD

PRD109,112002 (2024)

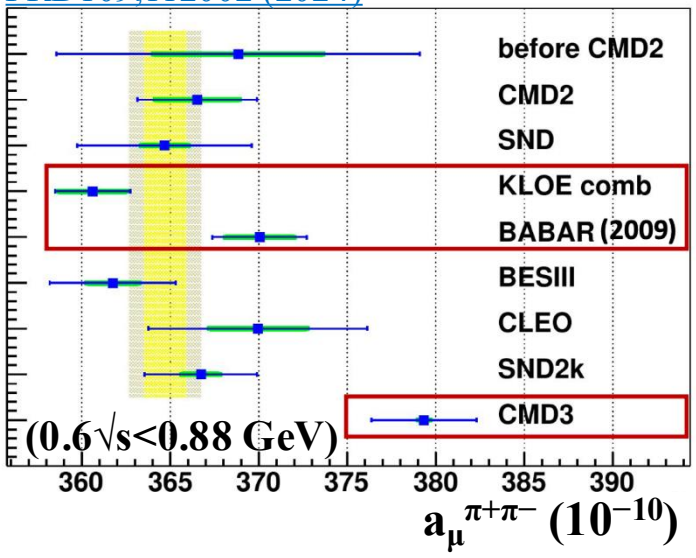

https://arxiv.org/pdf/2505.21476

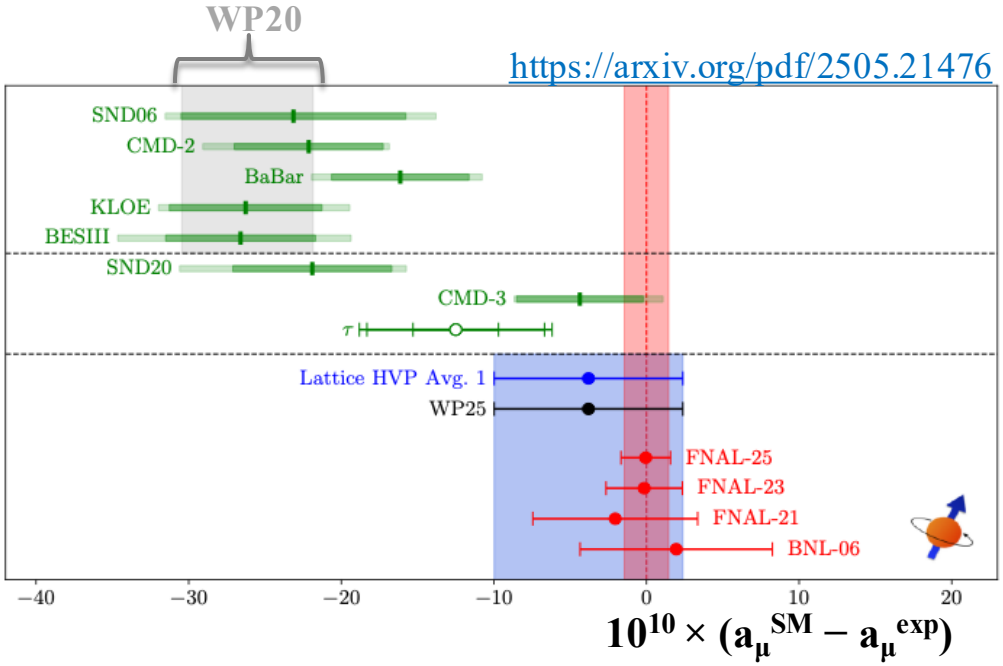

Current **tensions** also exist between:

- measurements from KLOE, BaBar and CMD-3 (KLOE vs CMD-3: >5σ tension at ρ peak)

CMD-3 Collaboration: PRD109,112002 (2024)
BaBar Collaboration: PRL103,231801 (2009)
KLOE Collaboration: PLB670, 285(2009), PLB700,102(2011), PLB720,336(2013)

The BaBar experiment

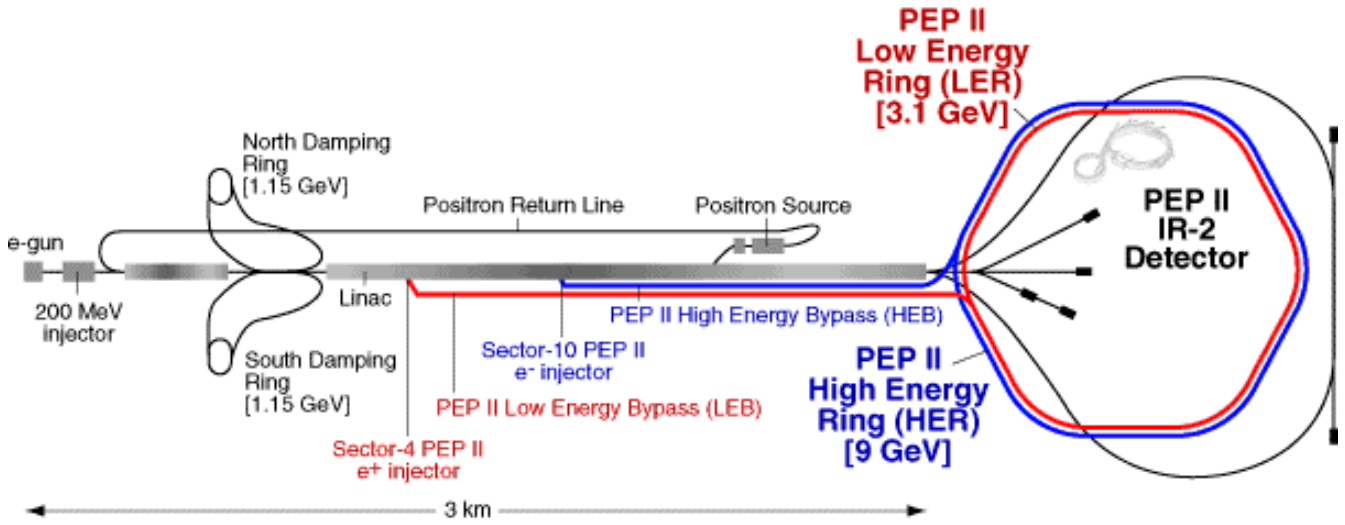

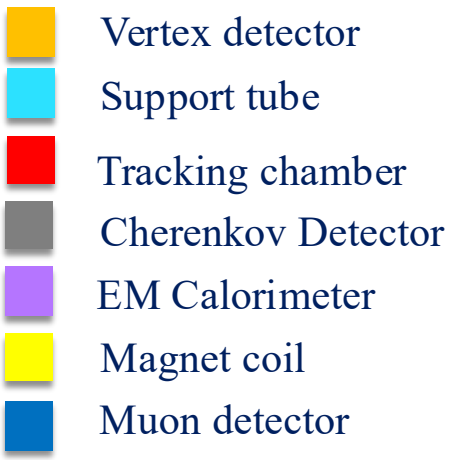

- Asymmetric e^+e^- collider operating at center-of-mass (cms) energy $\sqrt{s}$ close to 10.58 GeV
- Total integrated luminosity of 514 fb^{-1} collected, mostly at the $\Upsilon(4S)$ resonance (424.2 fb^{-1})
  - Initial-State-Radiation (ISR): the emission of a photon in the initial state allows to exploit a lower cms energy range, from threshold to $\sqrt{s}$

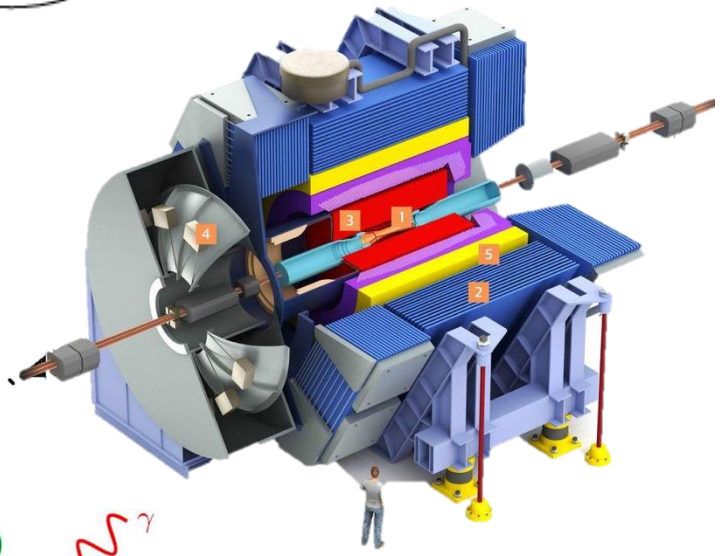

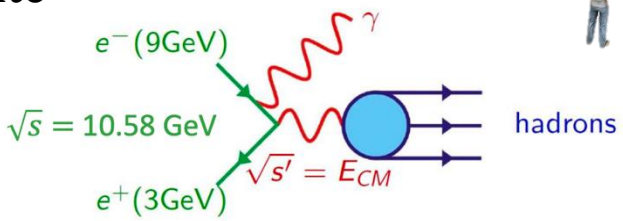

ISR Approach to Measuring $e^+e^- \to \pi^+\pi^-/\mu^+\mu^-$ Cross Section

Previous BaBar results from 2009 (partial data)

This talk: new BaBar measurement of $e^+e^- \to \gamma_{ISR}\,\pi^+\pi^-/\mu^+\mu^-$ cross section with full data samples plus & independent method aimed to improve precision

- γ_{ISR} is from Initial State Radiation
- Reduced energy: $s' = s\left(1 - \frac{2E^*_\gamma}{\sqrt{s}}\right)$

where E^*_γ is the ISR photon energy in the e^+e^- cms, and s the square of the e^+e^- beam energy

- Higher order radiation considered with additional γ at ISR and FSR levels
- MC signals: $\pi^+\pi^-\gamma_{ISR}(\gamma)$ & $\mu^+\mu^-\gamma_{ISR}(\gamma)$ with Phokhara9.1 generator

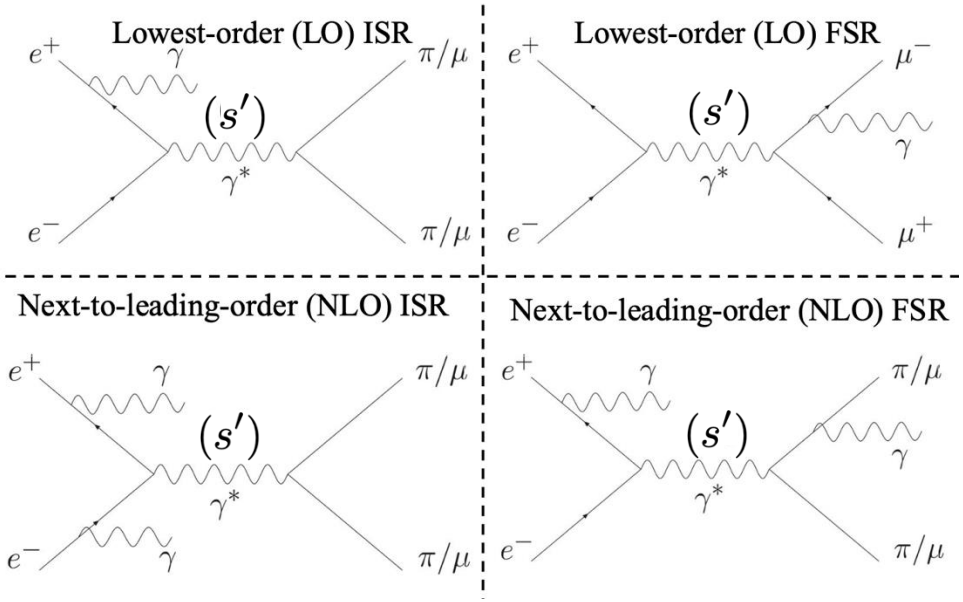

- MC backgrounds: $e^+e^- \to K^+K^-\gamma_{ISR}(\gamma)$, $q\bar{q}$ (q=u,d,s,c), $\tau^+\tau^-$, $X\gamma_{ISR}$ (X=nπ/K+mπ^0,...).

New Analysis: from the 2009 to the 2025 approach

2009 ANALYSIS PRL103,231801 (2009) PRD86,032013 (2012)

- Runs 1 to 4 (232 fb^{-1} at $\Upsilon(4S)$)

NEW 2025 ANALYSIS ➔ NEW METHOD

- Runs 1 to 6 (full data sample of 460 fb^{-1} at $\Upsilon(4S)$)

New Analysis: from the 2009 to the 2025 approach

2009 ANALYSIS PRL103,231801 (2009)

- Runs 1 to 4 (232 fb^{-1} at $\Upsilon(4S)$)
- Particle identification (PID) for π/μ separation → dominant systematic

NEW 2025 ANALYSIS → NEW METHOD

- Runs 1 to 6 (full data sample of 460 fb^{-1} at $\Upsilon(4S)$)
- **Removes explicit PID requirement and related systematic uncertainties**
- **Different method for π/μ separation:**
  - Uses different polar angle distributions of π and μ in c.m. frame arising from π being spin 0 and μ being spin 1⁄2

$$\frac{d\sigma}{d\cos\theta_\mu}(e^+e^- \to \mu^+\mu^-) \sim \beta_\mu[1+\cos^2\theta_\mu + (1-\beta_\mu^2)\sin^2\theta_\mu]$$

$$\frac{d\sigma}{d\cos\theta_\pi}(e^+e^- \to \pi^+\pi^-) \sim \sin^2\theta_\pi$$

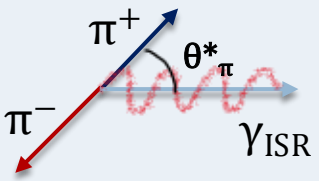

$\theta^*_{\pi/\mu}$ distributions in the ISR process follow the original polar angular distributions of the corresponding Born processes

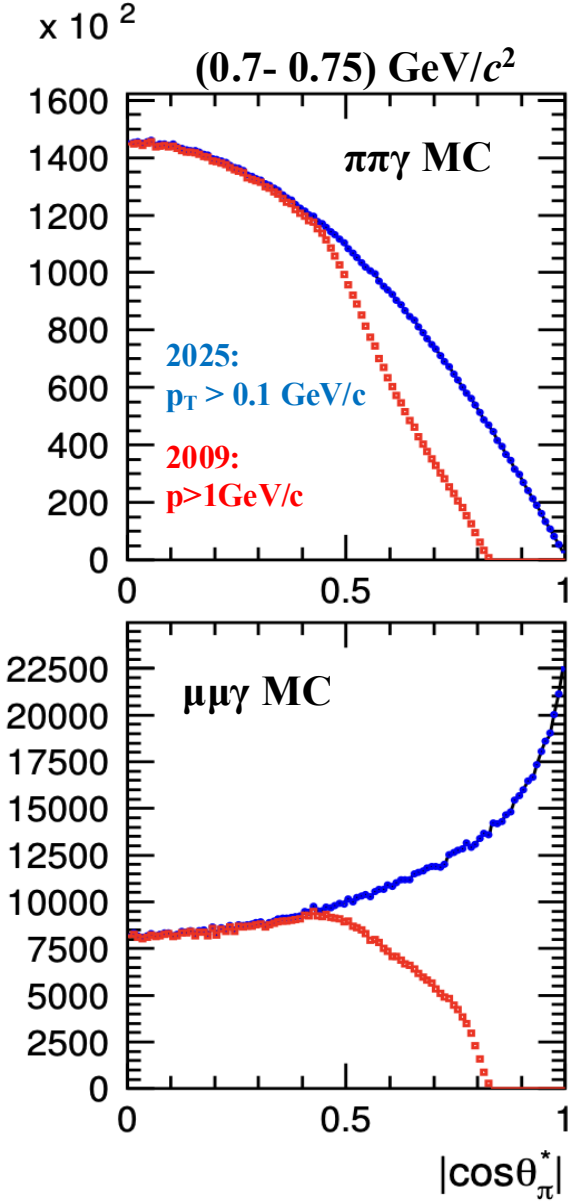

New Analysis: from the 2009 to the 2025 approach

2009 ANALYSIS PRL103,231801 (2009)

- Runs 1 to 4 (232 fb^{-1} at $\Upsilon(4S)$)
- Particle identification (PID) for π/μ separation → dominant systematic
- Selection of charged tracks with momentum p>1GeV/*c* (more reliable for μ-ID)

NEW 2025 ANALYSIS ➔ NEW METHOD

- Runs 1 to 6 (full data sample of 460 fb^{-1} at $\Upsilon(4S)$)
- **Removes explicit PID requirement and related systematic uncertainties**
- **Different method for π/μ separation:**
  - Uses different polar angle distributions of π and μ in cm frame arising from π being spin 0 and μ being spin 1⁄2
- Track $p_T > 0.1$ GeV/*c* (replaces p>1GeV/*c* requirement in 2009 analysis)

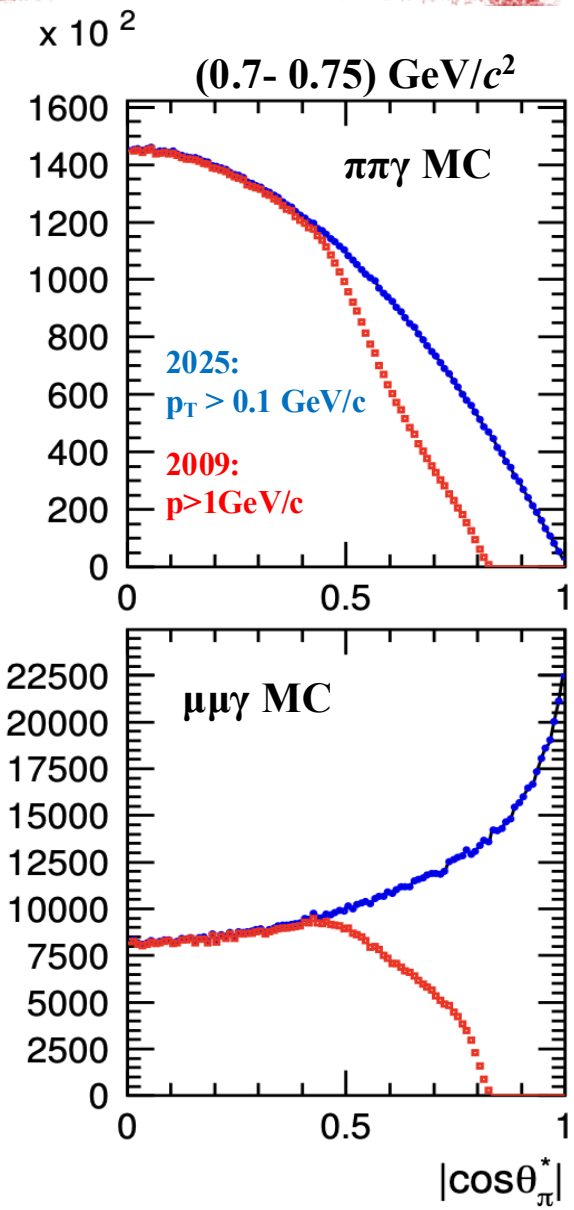

New Analysis: from the 2009 to the 2025 approach

2009 ANALYSIS PRL103,231801 (2009) PRD86,032013 (2012)

- Runs 1 to 4 (232 fb^{-1} at $\Upsilon(4S)$)
- Particle identification (PID) for π/μ separation → dominant systematic
- Selection of charged tracks with momentum p>1GeV/*c* (more reliable for μ-ID)
- Total relative systematic uncertainty (0.5-1 GeV/c^2) = 0.50%
- AfkQED generator for signal MC

NEW 2025 ANALYSIS → NEW METHOD

- Runs 1 to 6 (full data sample of 460 fb^{-1} at $\Upsilon(4S)$)
- **Removes explicit PID requirement and related systematic uncertainties**
- **Different method for π/μ separation:**
  - Uses different polar angle distributions of π and μ in cm frame arising from π being spin 0 and μ being spin 1⁄2
- Track $p_T > 0.1$ GeV/*c* (replaces p>1GeV/*c* requirement in 2009 analysis)
- NLO Phokhara9.1 generator for signal MC (+AfkQED for systematic studies)

- **Independent method to check 2009 BaBar results**
- **Blind analysis: offsets (constant multiplicative factors) applied on mass spectra at different steps**

Overview of Analysis procedure

1. **Kinematic fits:** for both $\mu\mu\gamma$ and $\pi\pi\gamma$ processes, the event definition is enlarged to include the radiation of one photon in addition to the already required ISR photon → 2-dimensional selection against background (slide 9)
2. **Angular fit** of data with data/MC correction → $\mu\mu$ and $\pi\pi$ mass spectra
   - **blinding** on absolute normalization of tracking corrections, trigger corrections and fitted mass spectra, independently for $\mu\mu$ and $\pi\pi$: 6 different blindings (slides 10 -12)
3. **Conclusive comparison** of **μμ** spectrum shape vs simulation → **unblinding of μμ** to compare normalization to QED prediction (slide 13)
4. **Successful QED test → μμ spectrum unfolded** to √s', i.e. center-of-mass energy of final state including Final State Radiation (FSR) → ISR luminosity (slide 14)
5. **ππ spectrum unfolded → cross section** in √s', blinded contribution to a_μ compute to first check uncertainties (slide 15)
6. **After extensive review and approval** from the Collaboration, **ππ cross section and contribution to a_μ are unblinded** (slide 16)

1. Kinematic fits

For both μμγ and ππγ processes, the event definition is enlarged to include the radiation of one photon in the addition to the already required γ_{ISR}

Large Angle (LA) fit: the additional γ is detected in the EMC, so the energy and angles are used in the fit. The extra γ can be either from FSR or from ISR at LA to the beams

Small Angle (SA) fit: the additional γ is assumed to be from ISR at small angle to the beams and undetected. The fit assumes this additional γ is perfectly aligned with either e^+e^- beams

DATA: **μμγ** (0.5<m<1 GeV/c^2)

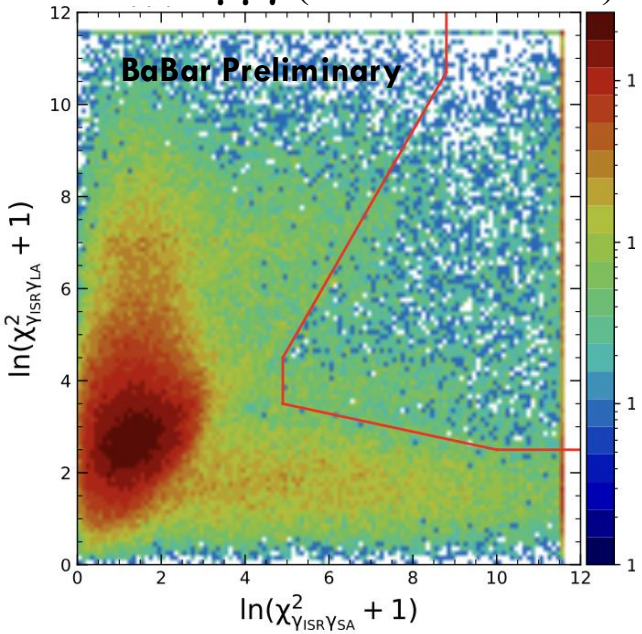

DATA: **ππγ** (0.5<m<1 GeV/c^2)

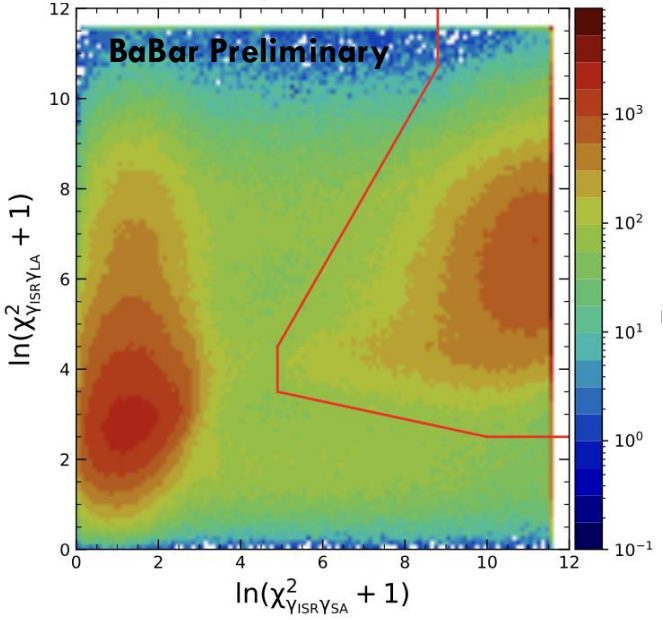

- Tails indicate events with additional radiation
- Larger background in ππγ process, suppressed with optimized BDT-based 2D-χ^2 selection (98-99% signal efficiency)

2. Angular fits

|cos(θ*)| fits on background-subtracted data distributions with

- templates of ***ππγ, μμγ,*** and ***KKγ*** obtained from MC simulation
- data-driven templates for ***eeγ*** process (no reliable simulation) using cut-based and BDT selections
- Templates need to be corrected for
  - trigger and tracking efficiencies corrections (blinded)
  - Vertex constraint V_{xy} selection efficiency
  - 2D-χ^2 selection efficiency

- Fit performed twice: in pion mass ($m_{\pi\pi}$) and muon mass ($m_{\mu\mu}$) charged track hypotheses to get both $\pi\pi\gamma$ and $\mu\mu\gamma$ spectra

- Data |cos(θ*)| distribution is adjusted by linear combination of templates in > 300 bins

- **3-step strategy for the fits ➔ reduces sensitivity to systematic uncertainty on data-drive eeγ determination**
  1. fit |cos(θ*)| in 0.9-1 to get normalization of eeγ
  2. fit |cos(θ*)| in 0-0.9 to separate $\pi\pi/\mu\mu$ (also KK for mass < 0.4 GeV/c^2, the normalized eeγ subtracted)
  3. Extrapolate to 1 to get full $\pi\pi/\mu\mu$ mass spectra

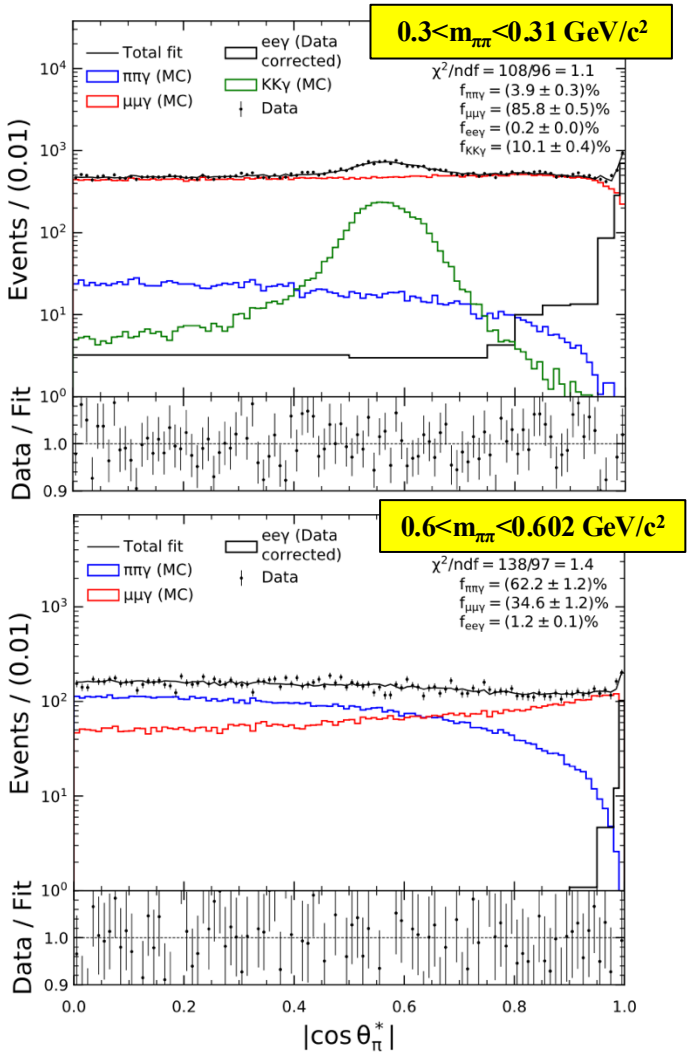

- Fit fraction (f_{xx}) extracted from template shapes ➔ Mass spectra blinded

2. Angular fits: Corrections to Templates and Mass Distributions

- Detailed and dedicated analysis studies of data/MC differences on PID-selected muon and pion sample: trigger, tracking, V_{xy}, and 2D-χ^2 selections
- Efficiency correction applied:

$$\varepsilon = \varepsilon_{\mathrm{MC}} \left(\frac{\varepsilon^{\mathrm{data}}_{\mathrm{trigger}}}{\varepsilon^{\mathrm{MC}}_{\mathrm{trigger}}}\right) \left(\frac{\varepsilon^{\mathrm{data}}_{\mathrm{tracking}}}{\varepsilon^{\mathrm{MC}}_{\mathrm{tracking}}}\right) \left(\frac{\varepsilon^{\mathrm{data}}_{V_{xy}}}{\varepsilon^{\mathrm{MC}}_{V_{xy}}}\right) \left(\frac{\varepsilon^{\mathrm{data}}_{\chi^2}}{\varepsilon^{\mathrm{MC}}_{\chi^2}}\right)$$

- Additional correction for pions: fake photons and secondary interactions
- **Blinded procedure**: offset on tracking and trigger corrections

Each correction has 2 components

- ✓ Template shape corrections (affect $\pi\pi/\mu\mu$ separation)
- ✓ Mass dependence correction (affect $\pi\pi$ and $\mu\mu$ spectra)

- Large effect on mass spectra (below ±5%) that tends to cancel out when combined
- Overall, the correction are rather flat → small impact

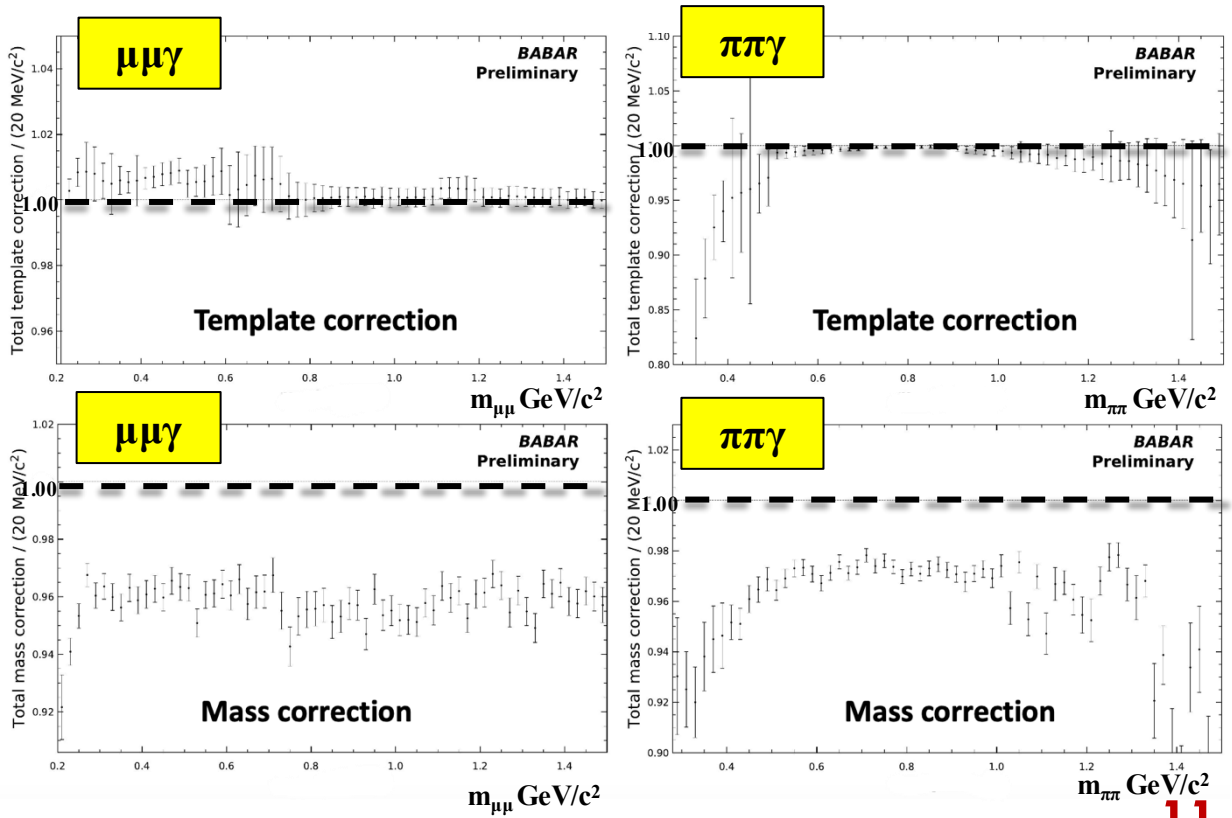

2. Angular fits: Fitted Mass Spectrum

- Mass spectra obtained from angular fit with corrected templates
- Masses also corrected for mass-dependent efficiencies
- Normalization of each spectrum initially blinded with a multiplicative factor. Here shown after unblinding
- Statistical errors computed with bootstrap method

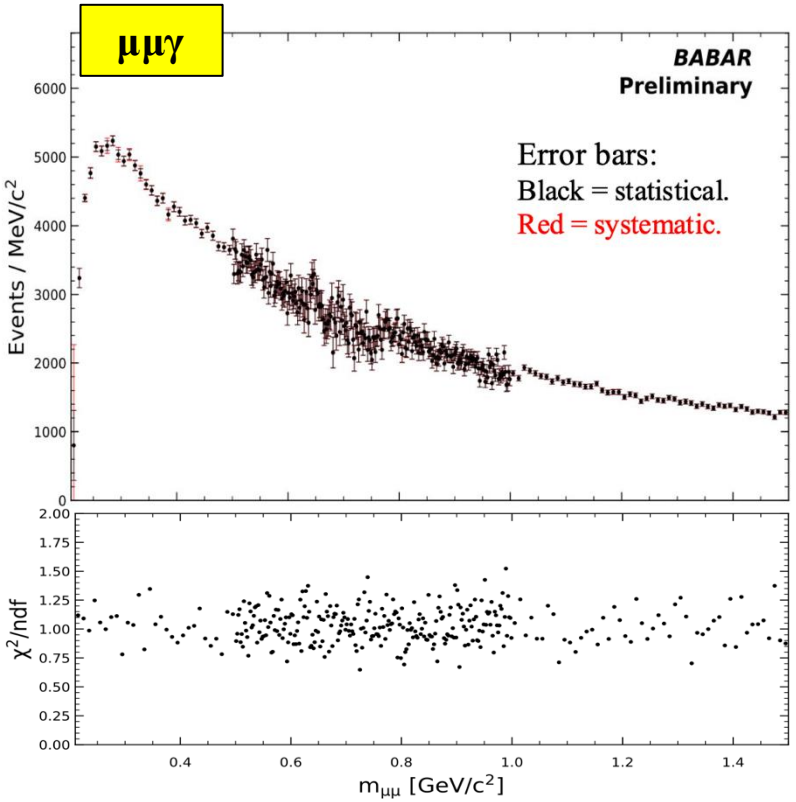

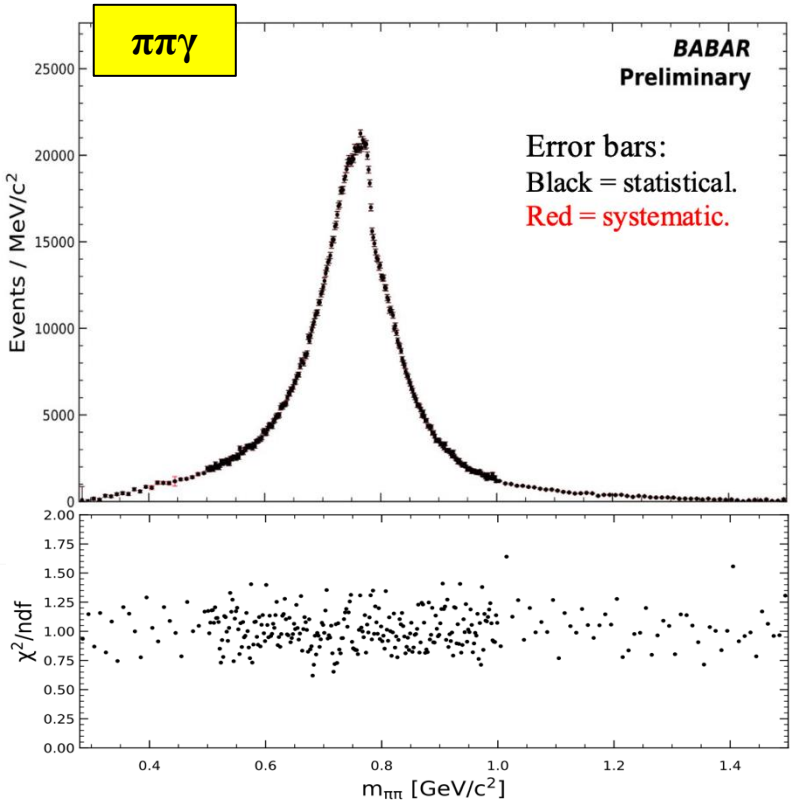

* bin width: 2 MeV/c^2 for 0.5-1.0 GeV/c^2; 10 MeV/c^2 elsewhere

3. μμγ Spectrum Comparison to QED prediction

$\mu\mu\gamma$ data spectrum can be compared to QED prediction, obtained by correcting the simulated *Phokhara* mass spectrum for:

- ISR photon efficiency
- shortcomings related to overestimation of ISR NLO and absence of NNLO in *Phokhara* [PRD108,L111103 (2023)]
- imprecise description of vacuum polarization effects

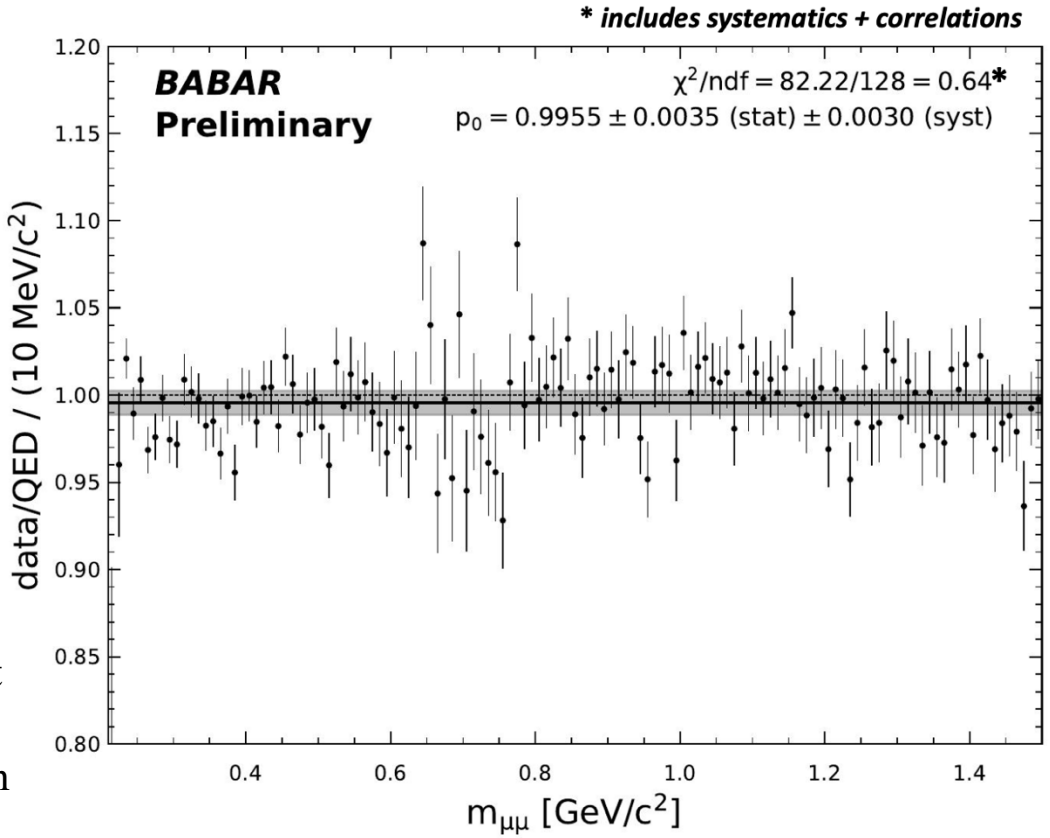

The data/QED ratio is fitted with a constant

- Agreement with QED within 0.71%
- Confirms robustness of ππ/μμ separation that does not introduce any systematic bias

$$R_{\mu\mu} = 0.9955 \pm 0.0035_{\text{stat}} \pm 0.0030_{\text{syst}} \pm 0.0033_{\gamma_{ISR}} \pm 0.0043_{\text{lumi}-ee}$$

- 0.0035_{stat}: data + stat uncertainty on corrections
- 0.0030_{syst}: Syst. uncertainty on corrections
- $0.0033_{\gamma_{ISR}}$: ISR photon data/MC efficiency
- $0.0043_{\text{lumi}-ee}$: Uncertainty on e^+e^- luminosity

4. Determination of ISR Luminosity

Effective ISR luminosity is determined from unfolded μμγ spectrum $dN^{\mathrm{ISR}}_{\mu\mu}/d\sqrt{s'}$

$$\frac{dL^{\mathrm{eff}}_{\mathrm{ISR}}}{d\sqrt{s'}} = \frac{dN^{\mathrm{ISR}}_{\mu\mu}/d\sqrt{s'}}{\epsilon_{\mu\mu}(\sqrt{s'})\,\sigma^{0}_{\mu\mu}(\sqrt{s'})}$$

acceptance of the selection (total efficiency) for muons

μμ bare cross section (without vacuum polarization) but including FSR contribution

4. Determination of ISR Luminosity

Effective ISR luminosity is determined from unfolded μμγ spectrum $dN^{\rm ISR}_{\mu\mu}/d\sqrt{s'}$

$$\frac{dL^{\rm eff}_{\rm ISR}}{d\sqrt{s'}} = \frac{dN^{\rm ISR}_{\mu\mu}/d\sqrt{s'}}{\epsilon_{\mu\mu}(\sqrt{s'})\sigma^0_{\mu\mu}(\sqrt{s'})} = \frac{dN^{\rm MC-gen}_{\mu\mu}}{d\sqrt{s'}} \times (1-f_{\rm LO\,FSR}) \times f_{\mu\mu}(\sqrt{s'}) \frac{1}{\sigma^0_{\mu\mu}(\sqrt{s'})}$$

- $\epsilon_{\mu\mu}(\sqrt{s'})$: acceptance of the selection (total efficiency) for muons
- $\sigma^0_{\mu\mu}(\sqrt{s'})$: μμ bare cross section (without vacuum polarization) but including FSR contribution
- $\frac{dN^{\rm MC-gen}_{\mu\mu}}{d\sqrt{s'}}$: Phokhara spectrum at generation level
- $(1-f_{\rm LO\,FSR})$: removes the small LO FSR contribution
- $f_{\mu\mu}(\sqrt{s'})$: 2nd order polynomial fit to data/MC

Unfolded μμγ spectrum replaced with a smooth function to mitigate the large stiatistical fluctuation ➔ justified by the successful QED test and slow/smooth variation of global template/mass corrections

4. Determination of ISR Luminosity

Effective ISR luminosity is determined from unfolded μμγ spectrum $dN^{\rm ISR}_{\mu\mu}/d\sqrt{s'}$

$$\frac{dL^{\rm eff}_{\rm ISR}}{d\sqrt{s'}} = \frac{dN^{\rm ISR}_{\mu\mu}/d\sqrt{s'}}{\epsilon_{\mu\mu}(\sqrt{s'})\sigma^0_{\mu\mu}(\sqrt{s'})} = \frac{dN^{\rm MC-gen}_{\mu\mu}}{d\sqrt{s'}} \times (1-f_{\rm LO\,FSR}) \times f_{\mu\mu}(\sqrt{s'}) \frac{1}{\sigma^0_{\mu\mu}(\sqrt{s'})}$$

- $\epsilon_{\mu\mu}(\sqrt{s'})$: acceptance of the selection (total efficiency) for muons
- $\sigma^0_{\mu\mu}(\sqrt{s'})$: μμ bare cross section (without vacuum polarization) but including FSR contribution
- $\frac{dN^{\rm MC-gen}_{\mu\mu}}{d\sqrt{s'}}$: Phokhara spectrum at generation level
- $(1-f_{\rm LO\,FSR})$: removes the small LO FSR contribution
- $f_{\mu\mu}(\sqrt{s'})$: 2nd order polynomial fit to data/MC

Unfolded μμγ spectrum replaced with a smooth function to mitigate the large stiatistical fluctuation ➔ justified by the successful QED test and slow/smooth variation of global template/mass corrections

Effective ISR Luminosity:

- small at low energy: larger statistical uncertainty there for processes with low cross section
- larger luminosity at higher energy, but ππ cross sections drop again there
- Two discontinuities due to the vacuum polarization contributions (included in Phokhara but not in the bare cross section)

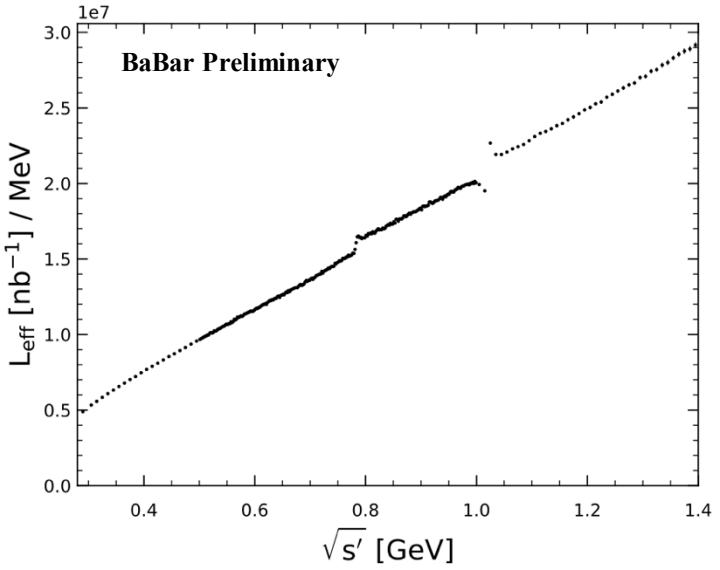

5. Measurement of $e^+e^- \to \pi^+\pi^-(\gamma)\gamma_{ISR}$ cross section

Bare cross section for ππ process is obtained from unfolded ππ spectrum using:

$$\sigma^0_{\pi\pi}(\sqrt{s'}) = \frac{dN_{\pi\pi}/d\sqrt{s'}}{\epsilon_{\pi\pi}(\sqrt{s'})\, dL^{\rm eff}_{\rm ISR}/d\sqrt{s'}} = \sigma^0_{\mu\mu}(\sqrt{s'}) \frac{dN_{\pi\pi}/d\sqrt{s'}}{dN^{\rm MC-gen}_{\mu\mu}/d\sqrt{s'} \times (1 - f_{\rm LO\,FSR}) \times f_{\mu\mu}(\sqrt{s'})} \frac{1}{\epsilon_{\pi\pi}(\sqrt{s'})}$$

- The bare cross section of the ππ process is the bare cross section of the μμ process weighted by the ratio of the unfolded data spectra of the ππ and μμ processes ➔ reduced systematic uncertainties due to the cancellation of the common error sources and corrections

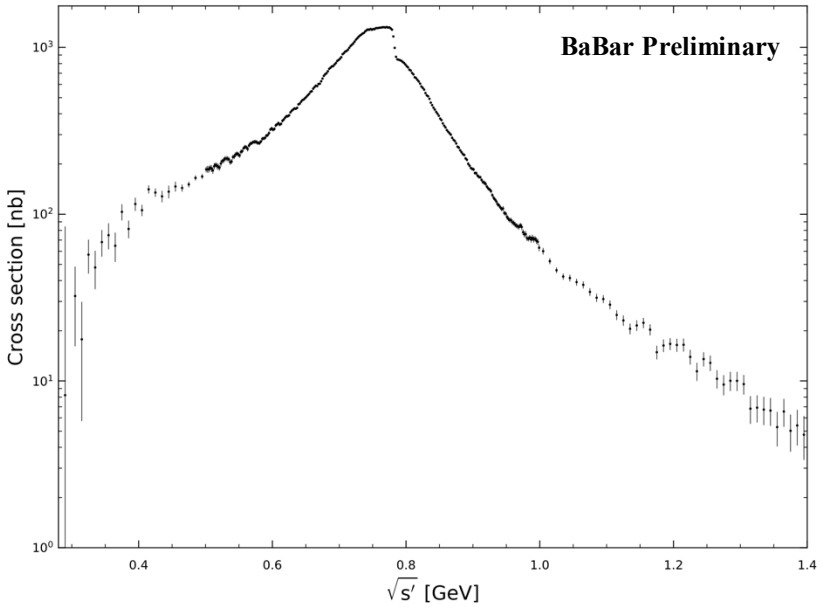

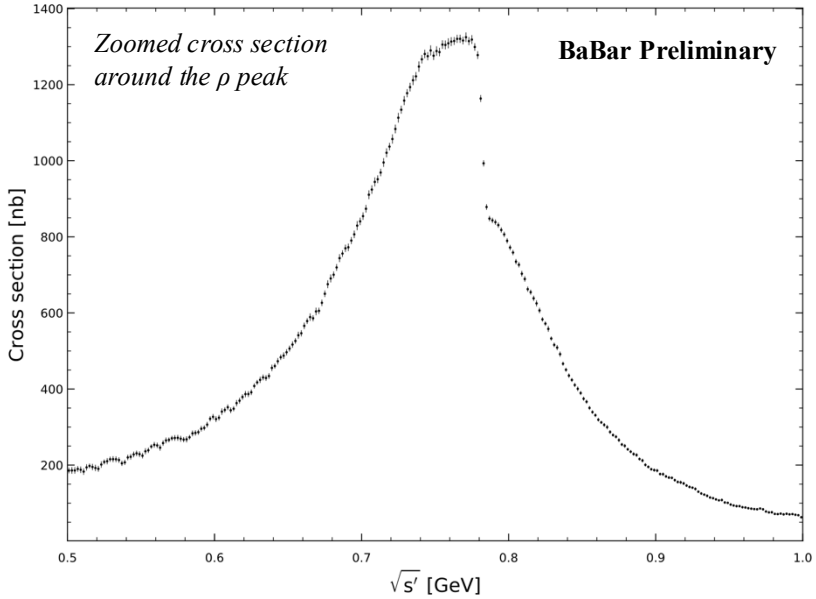

6. Comparison with 2009 BaBar result and contribution to a_μ

The 2025 cross section looks overall in good agreement with the previous measurement from 2009, except at large masses

$\pi\pi$ contributions to a_μ		
Energy range (GeV)	**2025** $a_\mu^{2\pi} \pm$ stat $\pm$ syst $[10^{-10}]$	**2009** $a_\mu^{2\pi} \pm$ stat $\pm$ syst $[10^{-10}]$
Below 0.5	58.0±5.5±1.7	58.2±0.6±0.6
0.5-1.4	456.2±2.2±1.7	455.6±2.1±2.6

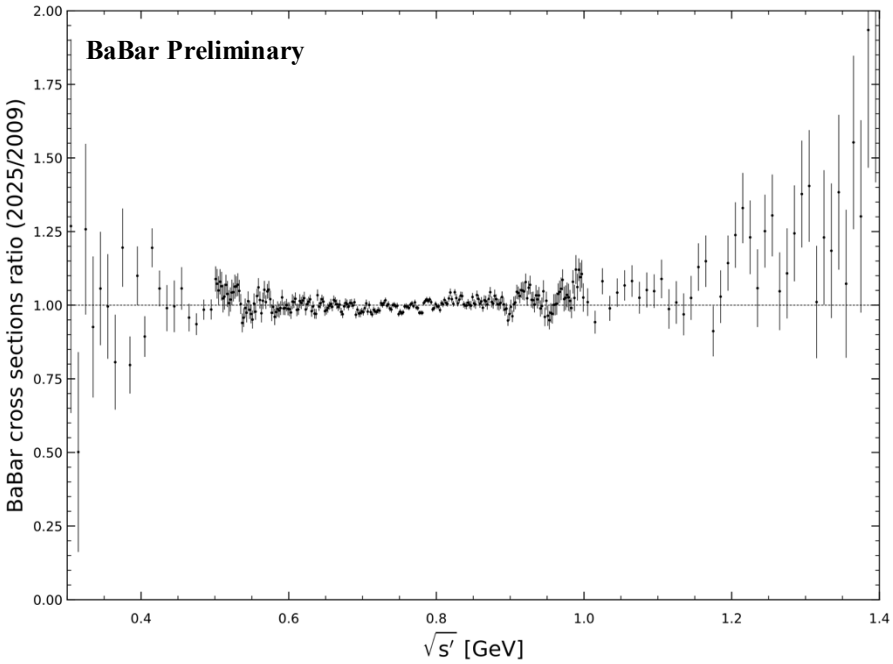

- Not competitive at low/high masses where μμ process dominates (more difficult ππ separation) but more precise in the ρ-peak region

- ✓ **2009** and **2025** results are **compatible** and in **excellent agreement** ➔ can be combined to provide the best precision of the BaBar measurement
- ✓ The averages yield the most precise $a_\mu^{2\pi}$ measurement from a single experiment

Energy range (GeV)	**2025-2009 average (preliminary)** $a_\mu^{2\pi}$ $[10^{-10}]$
Below 0.5	58.2±0.8
0.5 – 1.4	455.9±2.1
Below 1.4 (*sum considering correlations)	514.1±2.5
Below 1.8 (1.4 – 1.8 from 2009)	514.4±2.5

Summary and Conclusions

- Contribution of ππ channel to a_μ measured by BaBar via ISR in a new blind analysis, following an independent method from previous 2009 measuremnts with full data sample of around 460 fb^{-1}
- ππ and μμ separation carried out with fits of angular distributions. PID requirements removed in this work (dominant systematics in the 2009 study)
- Unblinded μμγ spectrum compared to QED prediction, showing compatibility with unity within uncertainties
- Unblinded ππγ cross section found to be in good agreement with 2009 measurement:

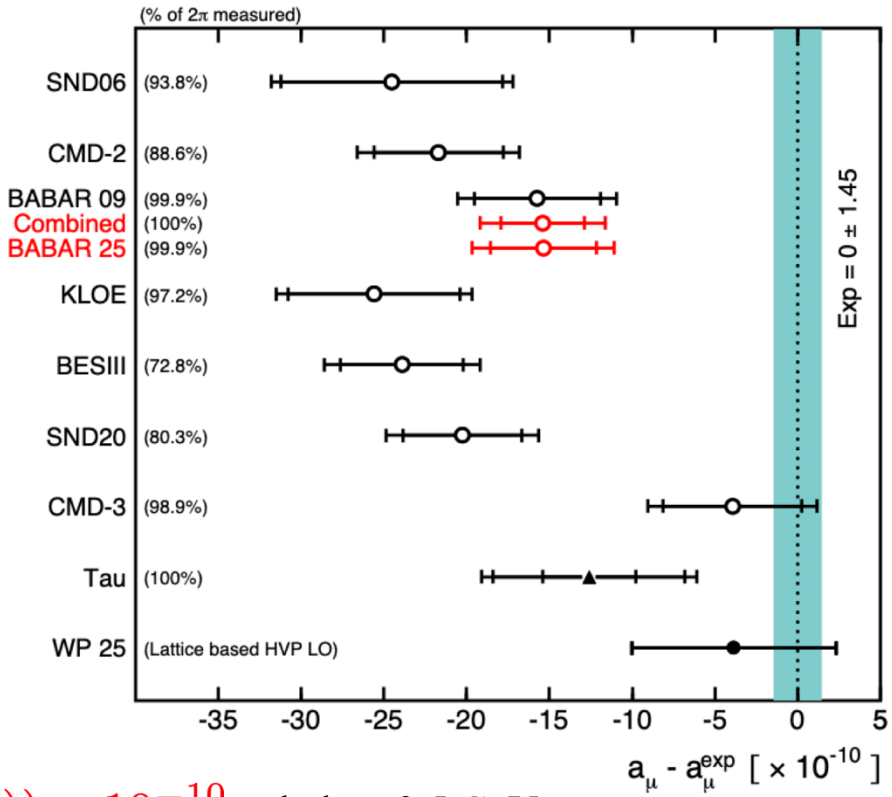

$$a_\mu^{2\pi,2025} = (58.0 \pm 5.5(\text{stat}) \pm 1.7(\text{syst})) \times 10^{-10}$$ below 0.5 GeV

$$a_\mu^{2\pi,2025} = (456.2 \pm 2.2(\text{stat}) \pm 1.7(\text{syst})) \times 10^{-10}$$ between 0.5 – 1.4 GeV

- Comparable statistical errors and reduced systematic uncertainties between 0.4-1.4 GeV (still preliminary)

This consistency obtained with an independent and fully blinded procedure shows the robustness of both analyses, which combined provide the most precise measurement of $a_\mu^{2\pi}$ from a single experiment

Back-up

BaBar Data sets

BABAR collected data from 1999-2008

- 432 fb^{-1} Υ(4S) "onpeak"
  (~470 x 10^6 BB pairs)
- 53 fb^{-1} non-resonant "offpeak"
  - collected ~40MeV below Υ(4S) peak
- Samples of "narrow Υ" events collected during last few months of running:
  - 122 x 10^6 Υ(3S) decays
  - 99 x 10^6 Υ(2S) decays

Process	Cross section (nb)
$b\bar{b}$	1.1
$c\bar{c}$	1.3
light quark $q\bar{q}$	~2.1
$\tau^+\tau^-$	0.9
e^+e^-	~40

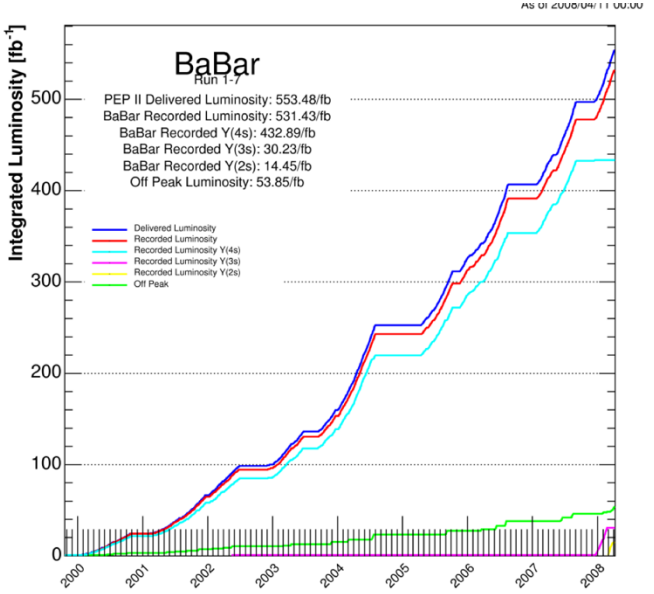

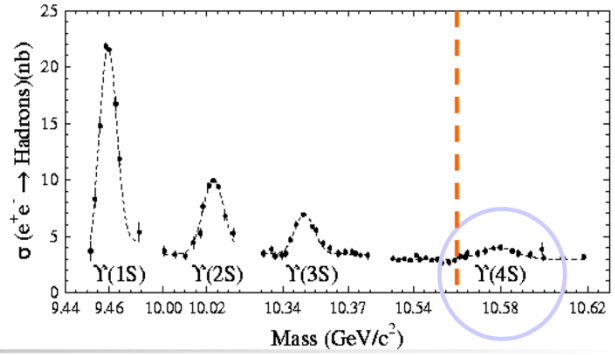

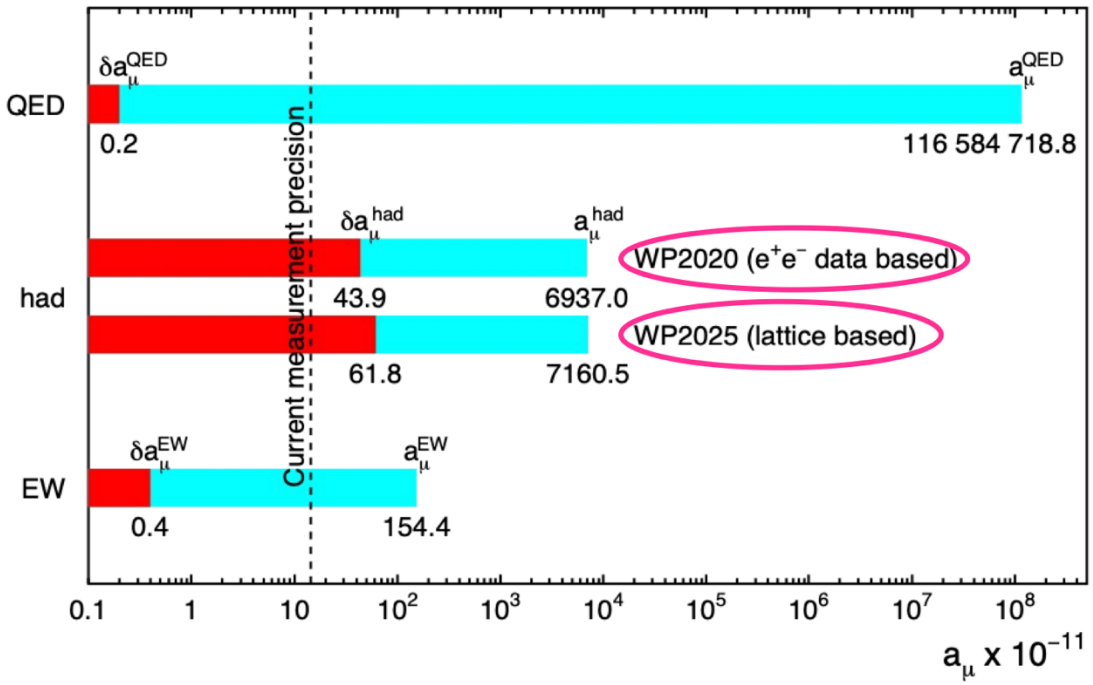

$$a_\mu^{\text{had}} = a_\mu^{\text{HVP LO}} + a_\mu^{\text{HVP HO}} + a_\mu^{\text{HLbL}}$$

had	HVP LO	HVP HO	HLbL
	$a_\mu[10^{-11}]$ (unc)		
WP2020	6931 (40)	−85.9 (0.7)	92 (18)
WP2025	7132 (61)	−87.2 (1.3)	115.5 (9.9)

WP2020: Phys. Rept. 887 (2020) 1
WP2025: arXiv:2505.21476

WP stands for the white paper of the muon g-2 theory initiative

e^+e^- Data-Based HVP Calculation

Based on analyticity and unitarity, the LO HVP contribution can be calculated using the dispersion relation [1] over $e^+e^- \rightarrow$ hadrons cross sections

$$a_\mu^{\text{HVP LO}} = \frac{\alpha^2}{3\pi^2}\int_{4m_\pi^2}^{\infty} ds \frac{K(s)}{s} R(s)$$

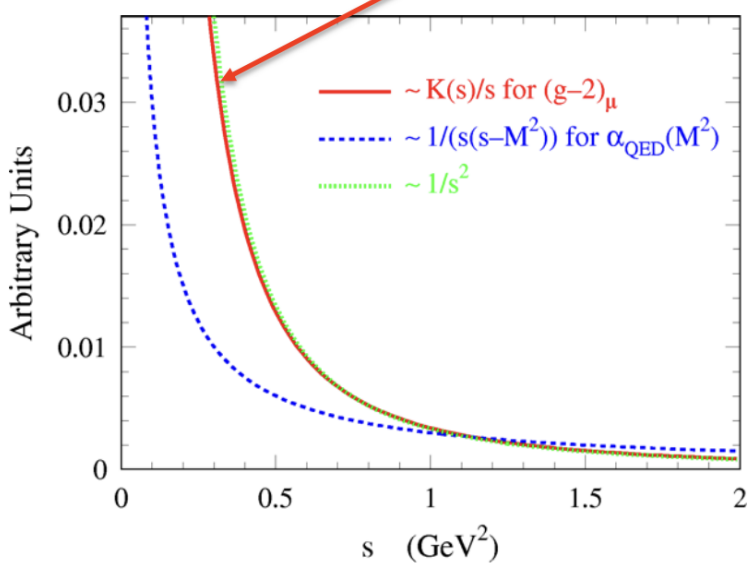

Bare: $\sigma^{(0)}(s) = \sigma(s)(\alpha/\alpha(s))^2$

$$12\pi\ \mathrm{Im}\Pi_\gamma(s) = \frac{\sigma^0\ [e^+e^- \rightarrow \text{hadrons}\ (\gamma_{FSR})]}{\sigma_{pt}} \equiv R(s)$$

Im[ ] ∝ | hadrons |²

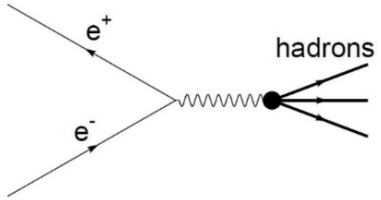

The QED kernel K(s) [2] has such an *s* dependence that low energy data contribute most:

➜ The precision is driven by that of $e^+e^- \rightarrow$ hadrons

[1] Bouchiat and Michel, 1961
[2] Brodsky, de Rafael, 1968

https://arxiv.org/pdf/2505.21476

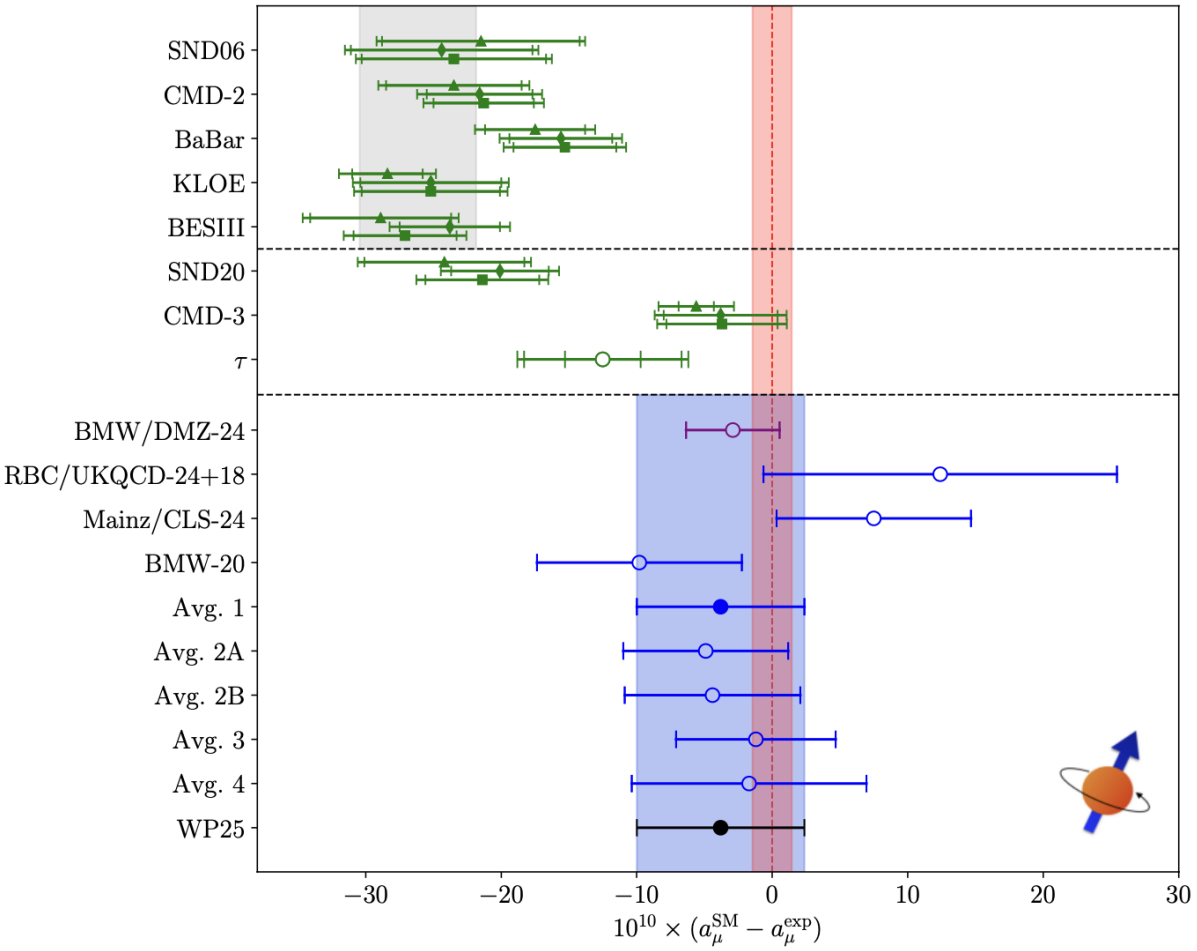

Figure 40: Final summary of various determinations of $a_\mu^{\rm HVP,\,LO}$ discussed in Secs. 2 and 3, propagated to $a_\mu^{\rm SM}$. The first two panels refer to data-driven determinations, where the three points for each e^+e^- experiment reflect the "CHKLS," "DHMZ," and "KNTW" methods, see Figs. 26 and 27 for more details. The gray band indicates the WP20 result, based on the e^+e^- experiments above the first dashed line. The τ point corresponds to Eq. (2.23). The last panel summarizes lattice-QCD determinations, including the hybrid evaluation [24], the three individual lattice-QCD calculations shown in Fig. 36, and the five lattice HVP averages from Fig. 37. The blue band refers to the final WP25 result, which coincides with "Avg. 1." In all cases, except for the gray WP20 band, the remaining contributions to $a_\mu^{\rm SM}$ beyond $a_\mu^{\rm HVP,\,LO}$ are taken from WP25, as given in Table 1. The red band denotes the experimental world average, which has been updated including the final results from the Fermilab experiment.

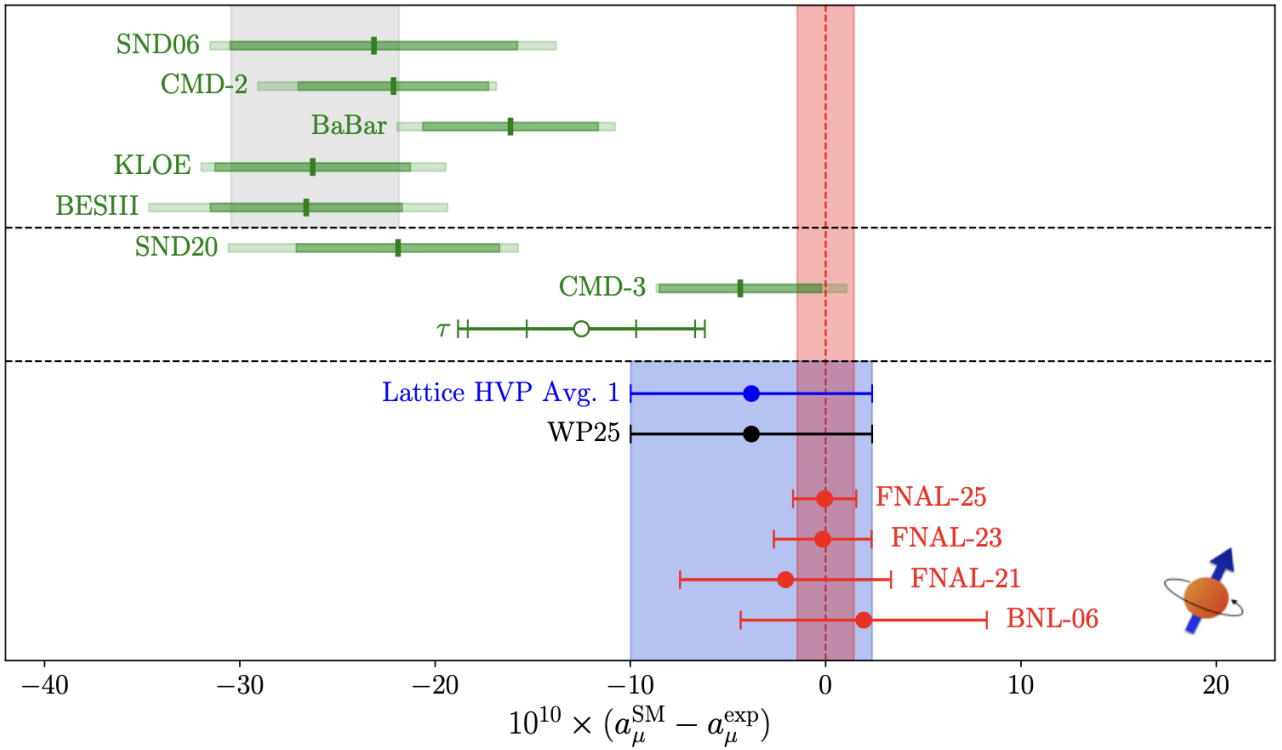

Figure 83: Summary of the current SM prediction for a_μ in comparison to experiment (red band and data points). The final WP25 prediction is denoted in black and via the blue band, it derives from the LO HVP result defined by the lattice-QCD "Avg. 1" shown in blue, see Eq. (3.37). The gray band indicates the WP20 result, based on the e^+e^- experiments above the first dashed line. These experimental ranges, as well as the ones for SND20 and CMD-3 that appeared after WP20, are produced as in Fig. 27; they are meant to illustrate the current situation, but cannot be interpreted as uncertainties with a proper statistical meaning. The τ point refers to Eq. (2.23), the numerical results are collected in Table 5. In all cases except for the gray WP20 band the LO HVP results are combined with WP25 values for the remaining contributions, as summarized in Table 1. The figure has been updated after the announcement of the final results from the Fermilab experiment, including the corrections to the previous experimental points as detailed in Ref. [8].

Unfolding procedure (mass spectrum ➔ √s′ energy spectrum)

Figure 43 (left)

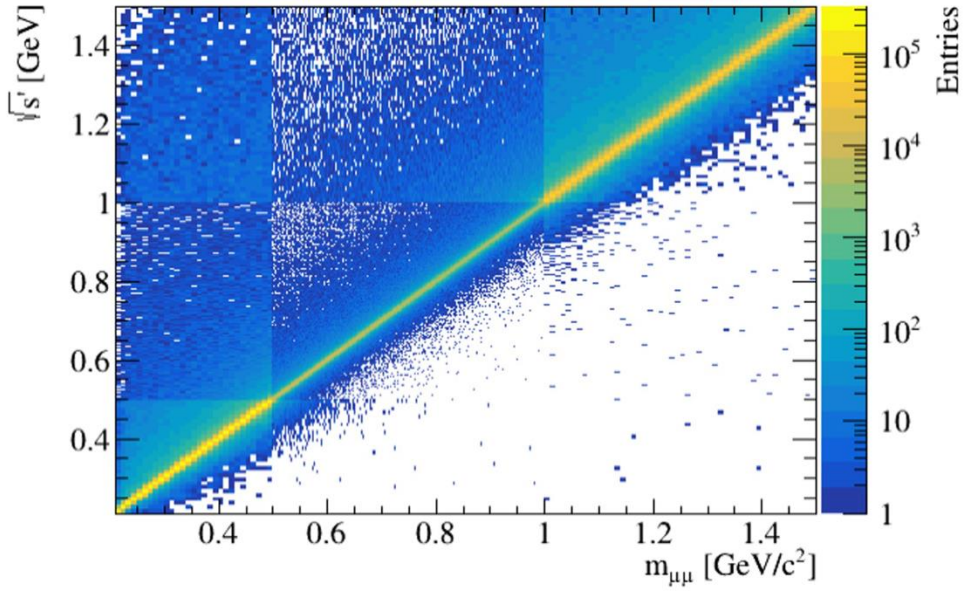

- To correct for
  - the detector resolution effect (small for muons given its relatively flat distribution)
  - the effect of including FSR photon (mass → √s′)
- Employ iterative unfolding procedure to account for data/MC shape difference
- Data-driven study of syst uncertainties, found to be small
- The block structure is due to different binnings and selections
- The asymmetric tail is due to the mass to √s′ change

cos θ* distributions for different mass ranges

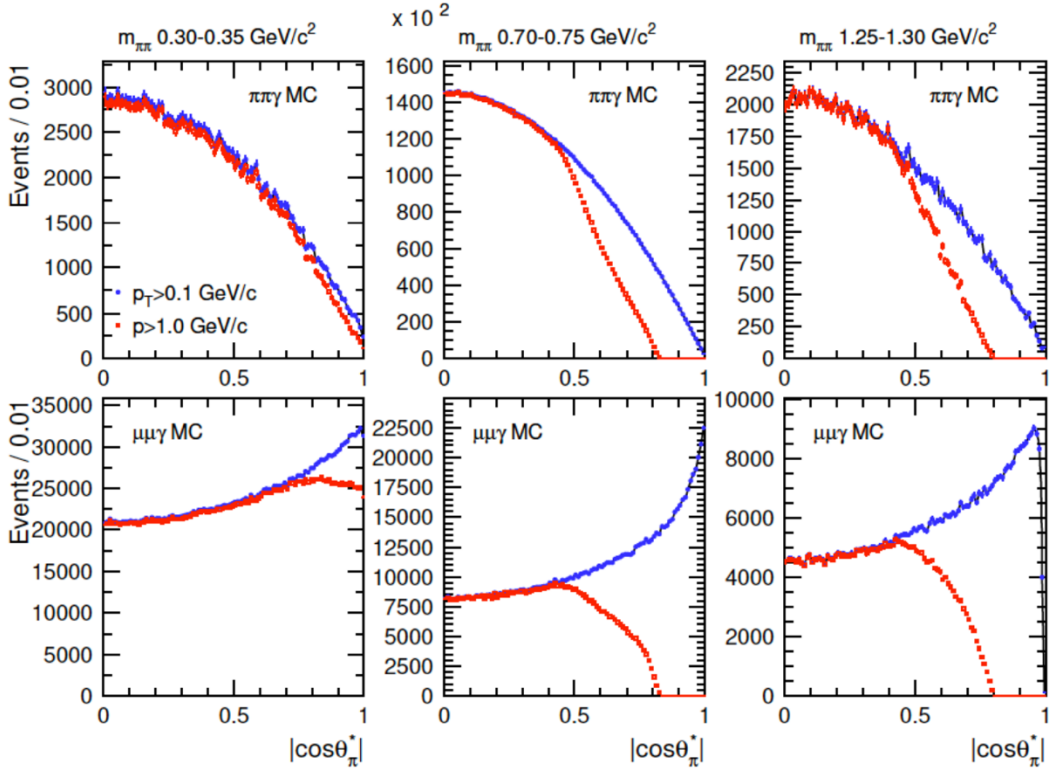

Figure 3: The $|\cos\theta^*_\pi|$ distributions in three mass intervals for $\pi\pi\gamma$ (top) and $\mu\mu\gamma$ (bottom) MC events within the geometrical acceptance selections, without momentum selection (black histogram), and different threshold values: $p > 1.0\,\mathrm{GeV/c}$ (red, 2009 analysis) and $p_T > 0.1\,\mathrm{GeV/c}$ (blue, this analysis).